Supplemental data

Genome-wide analysis of the spatiotemporal regulation of firing and dormant replication origins in human cells

Nozomi Sugimoto[1,*], Kazumitsu Maehara[2], Kazumasa Yoshida[1], Yasuyuki Ohkawa[2] and Masatoshi Fujita[1,*]

[1] Department of Cellular Biochemistry, Graduate School of Pharmaceutical Sciences, Kyushu University, 3-1-1 Maidashi, Higashiku, Fukuoka 812-8582, Japan
[2] Division of Transcriptomics, Medical Institute of Bioregulation, Kyushu University, 3-1-1 Maidashi, Higashiku, Fukuoka 812-8582, Japan

* To whom correspondence should be addressed. Tel: +81-92-642-6637; Fax: +81-92-642-6635; Email: sugimoto@phar.kyushu-u.ac.jp and mfujita@phar.kyushu-u.ac.jp

SUPPLEMENTAL FIGURE LEGENDS

Supplemental Figure S1. Quality control of MCM7 ChIP-Seq analysis.

(A) HeLa cells were transfected with control (mixture of siLuci and siGFP) or MCM7 (mixture of MCM7-2 and -3) siRNAs for 48 h using Lipofectamine RNAiMAX (Invitrogen) according to the manufacturer's instructions, and subjected to immunoblotting using anti-MCM7 antibody (29). siRNA oligonucleotides were synthesised by IDT as follows (sense strand):

siMCM7-2 (5'-AGAUGCAAGAACAUAGUGAUCAGdGdT-3'),

siMCM7-3 (5'-GGCGGCUCUGGAUGAAUAUGAGGdAdG-3').

Sequences of siLuci and siGFP controls were previously reported (28). Relative amounts of MCM7 are shown below. (B) ChIPed DNA analysis by SYBR Gold staining and UV imaging. 1–3, standard DNAs. 4–7, co-precipitated DNAs prepared from HeLa cells transfected with control (mixture of siLuci and siGFP) or MCM7 (mixture of siMCM7-2 and -3) siRNAs for 48 h with anti-MCM7 antibody or control rabbit IgG. (C) The amount of co-precipitated DNA was semi-quantified using standard DNA and input DNA using a UV spectrometer. (D) The number of MCM7_1st_wo0.5_SNS peaks within 0.5 kb of MCM7_2nd_wo0.5_SNS peaks is significantly higher than that obtained with shuffled MCM7_1st_wo0.5_SNS peaks. * indicates $p < 0.0001$ by Chi-square test. (E) Aggregation plots showing the localisation of MCM7_2nd_wo0.5_SNS peaks and shuffled peaks surrounding MCM7_1st_wo0.5_SNS peaks.

Supplemental Figure S2. Analyses of firing and dormant origins classified with original SNS-Seq data.

(A) Selected snapshots of the genome browser view around the *LMNB2*, *MCM4*, and *MYC* loci. Visual representations of sMCM7, SNS-Seq (12, 13), and Ini-Seq (40) data are shown. Green lines indicate

known origin regions. (B) Venn diagram showing overlap (within 0.5 kb) of sMCM7 and original SNS-Seq peaks (12). (C) The number of sMCM7 peaks within 0.5 kb of the SNS peaks is significantly higher than that obtained with shuffled sMCM7 peaks. * indicates $p < 0.0001$ by Chi-square test. (D) Aggregation plots showing the localization of the SNS peaks and shuffled peaks surrounding sMCM7 peaks. (E) Aggregation plots showing FAIRE-Seq signals surrounding the indicated origin classes. (F) Aggregation plots showing the signals of MCM7_1st ChIP-Seq surrounding the indicated origin classes. (G) Firing and dormant origin sites were aggregated together with TSS sites.

Supplemental Figure S3. Analyses of firing and dormant origins classified with Ini-Seq data.

(A) Venn diagram showing overlap (within 0.5 kb) of sMCM7 and Ini-Seq peaks (40). (B) The number of sMCM7 peaks within 0.5 kb of Ini-Seq peaks is significantly higher than that obtained with shuffled sMCM7 peaks. * indicates $p < 0.0001$ by Chi-square test. (C) Aggregation plot showing the localization of Ini-Seq peaks (40) and shuffled peaks surrounding sMCM7 peaks. (D) Aggregation plots showing FAIRE-Seq signals surrounding the indicated origin classes. (E) Aggregation plots showing the signals of MCM7_1st ChIP-Seq surrounding the indicated origin classes. (F) Firing and dormant origin sites were aggregated together with TSS sites. (G) GC content of 10,000 randomly selected origins. Grey boxes represent results obtained using shuffled datasets. The Wilcoxon rank sum test was used to calculate *p*-values. (H) Aggregation plots of G4-Seq peaks surrounding firing and dormant origins.

Supplemental Figure S4. Additional properties of firing and dormant origins.

(A) Aggregation plots showing ChIP-Seq signals of MCM7_2nd surrounding the indicated origin classes (left). Cumulative MCM7_2nd ChIP-Seq signals surrounding firing or dormant origins (±1 kb from the centre of each peak) are also shown (right). (B) Aggregation plots showing FAIRE-Seq signals surrounding the indicated histone markers. (C) Averaged profiles of sMCM7 at all genes were calculated to assess the distribution of these sites on genes. Marks -5 kb and +5 kb indicate 5kb upstream of TSSs and 5 kb downstream of TES, respectively.

Supplemental Figure S5. Comparison of correlation between various MCM ChIP-Seq data and SNS or Ini-Seq data.

(A-E) Venn diagram showing the overlap (within 0.5 kb) of MCM peaks from different datasets and SNS (left) or Ini-Seq (right) peaks in HeLa cells. For data sources, see Supplemental Table S1. (A) These are same as Figure 1E and Supplemental Figure S3A. (B) Original MCM2 ChIP-Seq data were obtained from Cucco et al. (38). (C) Because the number of the original MCM2 ChIP-Seq peaks appears small compared with our MCM7 peaks, we also investigated the re-analysed MCM2 peaks obtained with peak detection and identification method we used for MCM7 (see Materials and Methods). (F-H) Venn diagram showing the overlap (within 0.5 kb) of MCM peaks and SNS peaks in K562 cells. For data sources, see Supplemental Table S1.

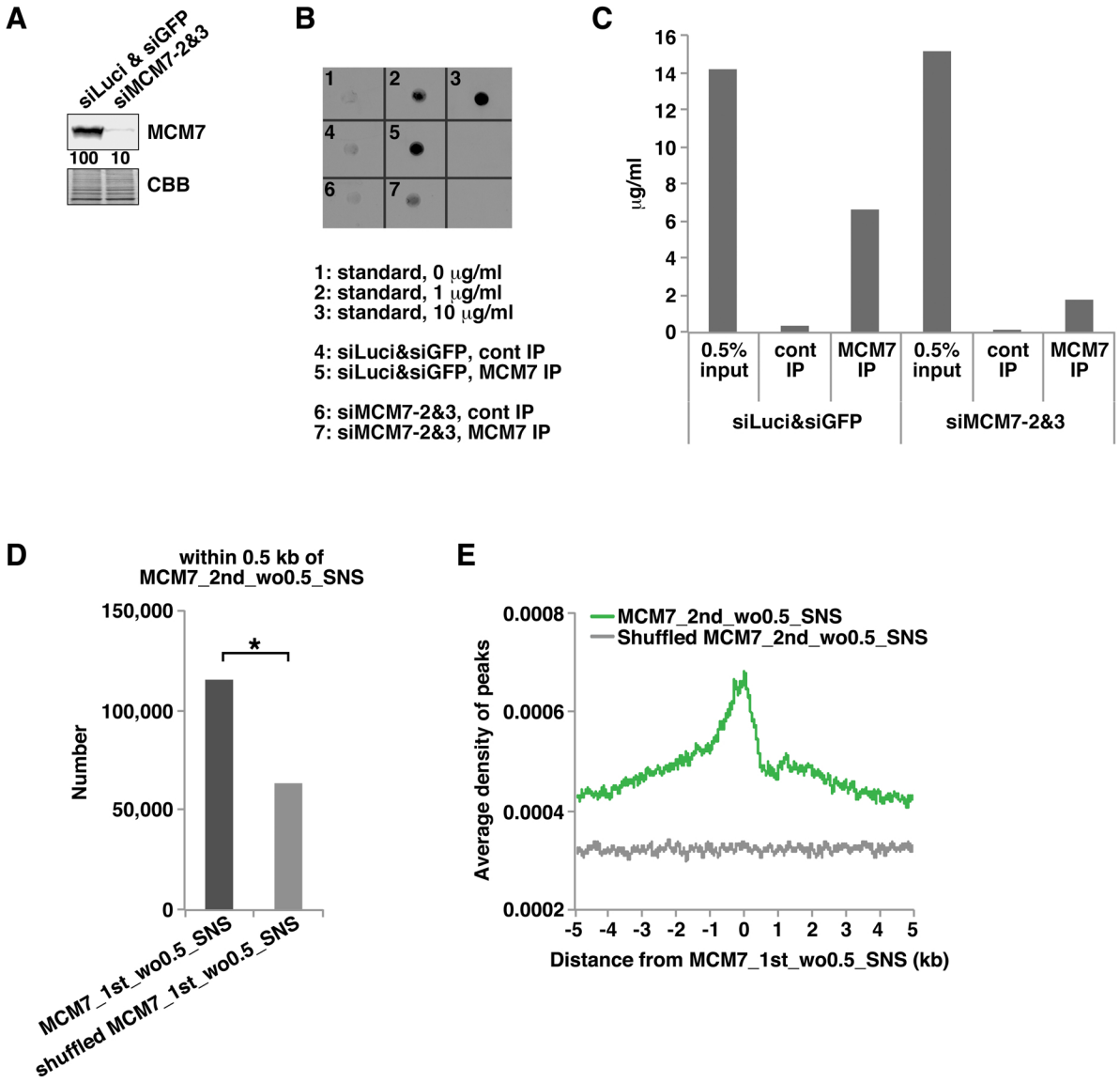

Supplemental Figure S1
Sugimoto et al.

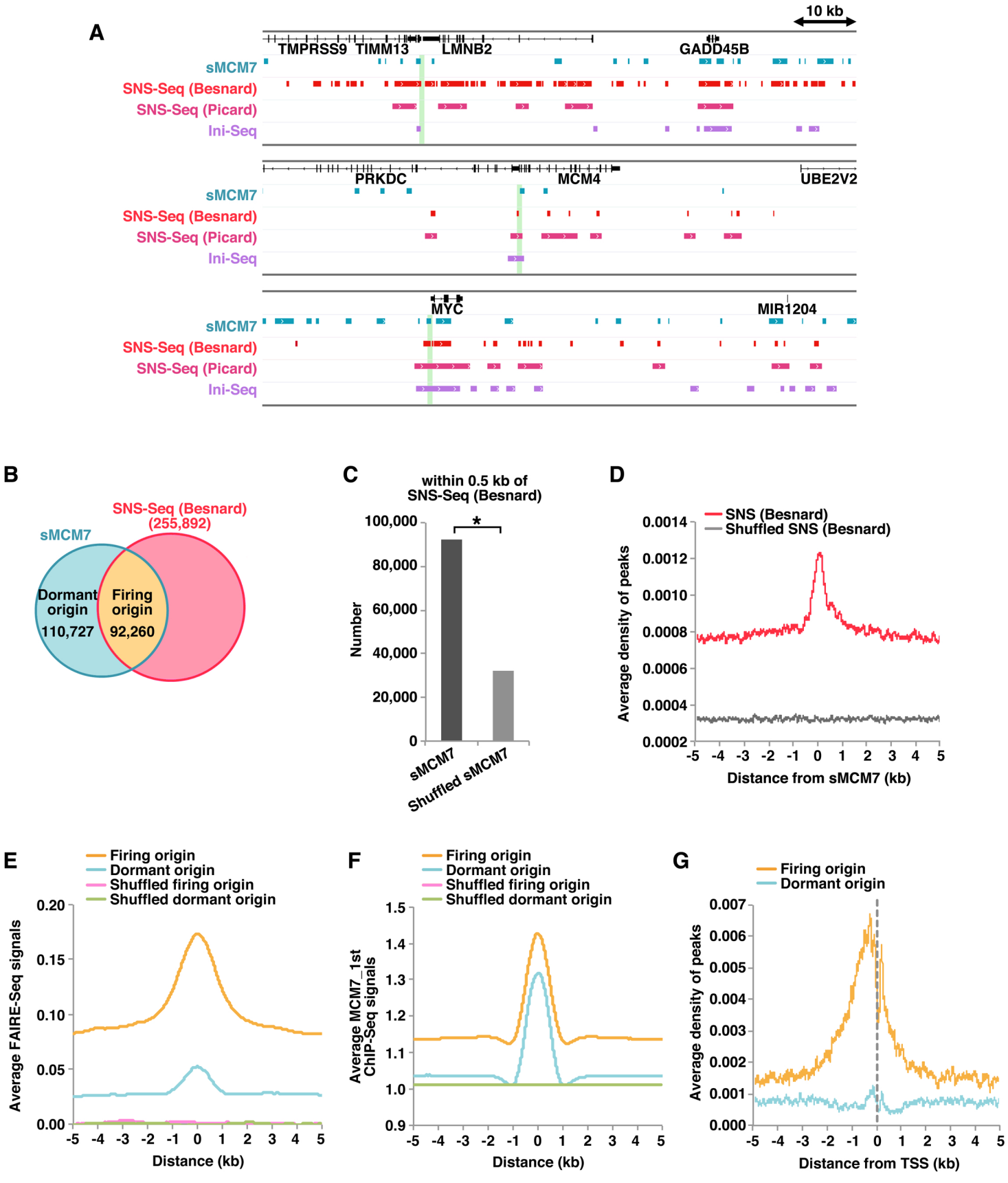

Supplemental Figure S2
Sugimoto et al.

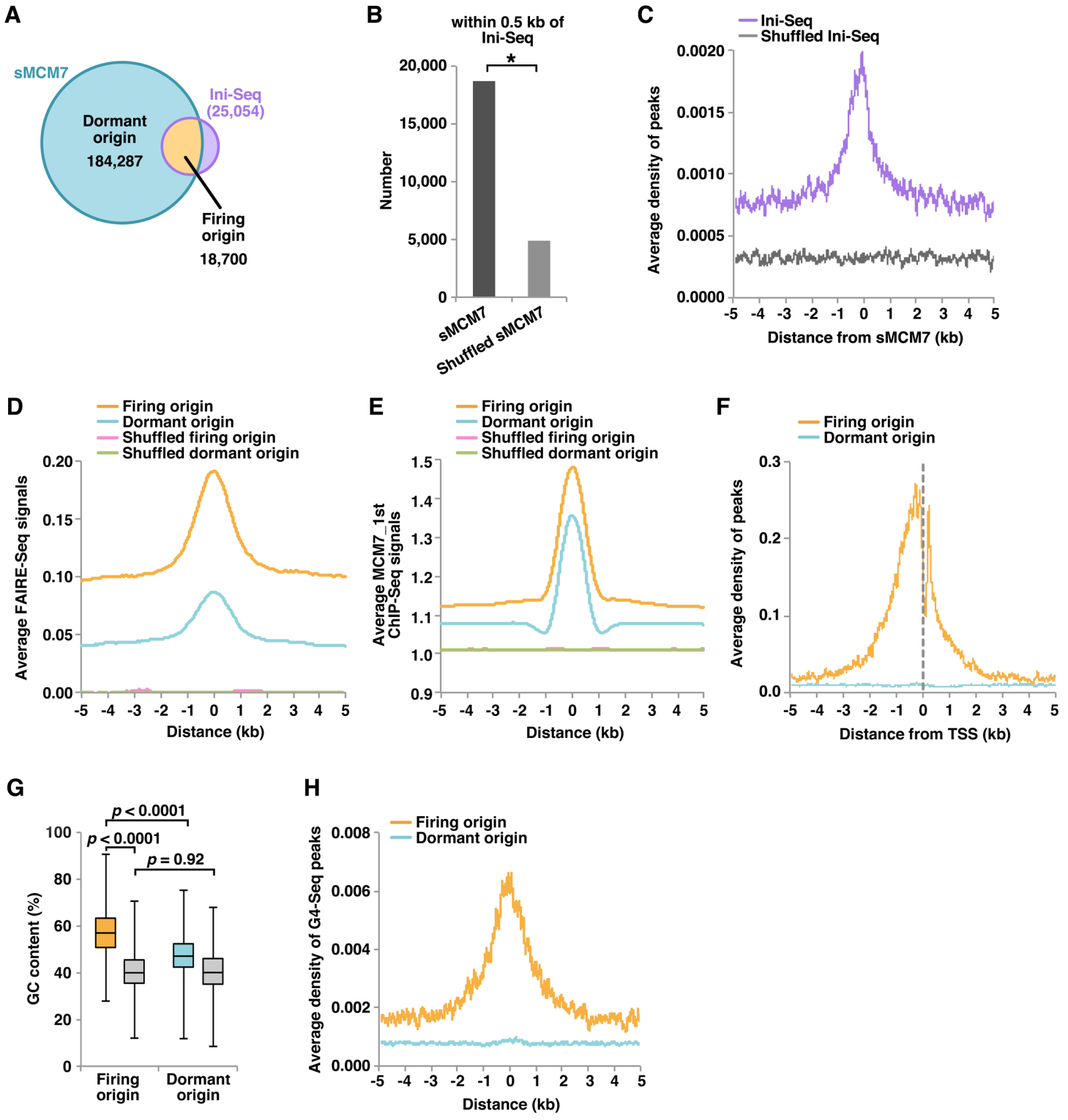

Supplemental Figure S3
Sugimoto et al.

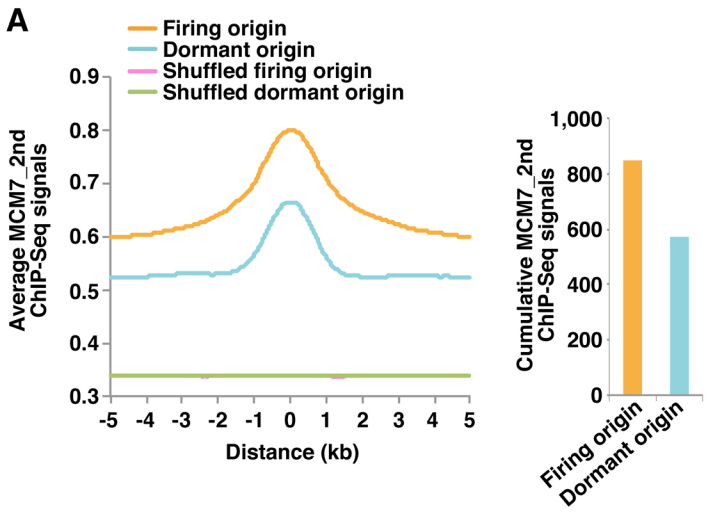

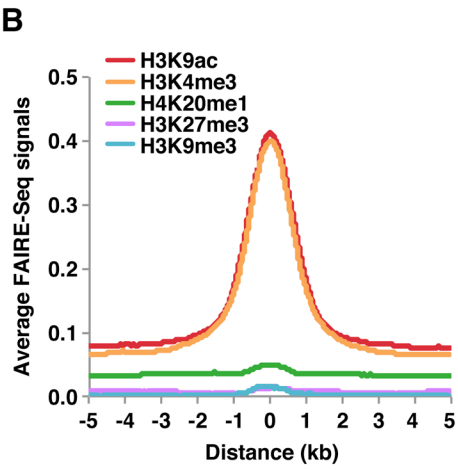

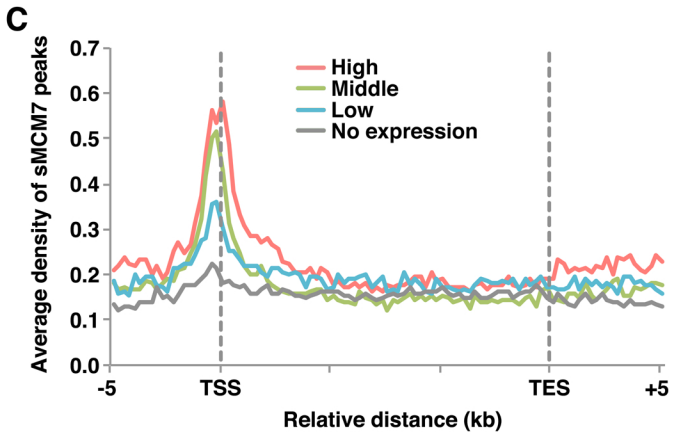

Supplemental Figure S4
Sugimoto et al.

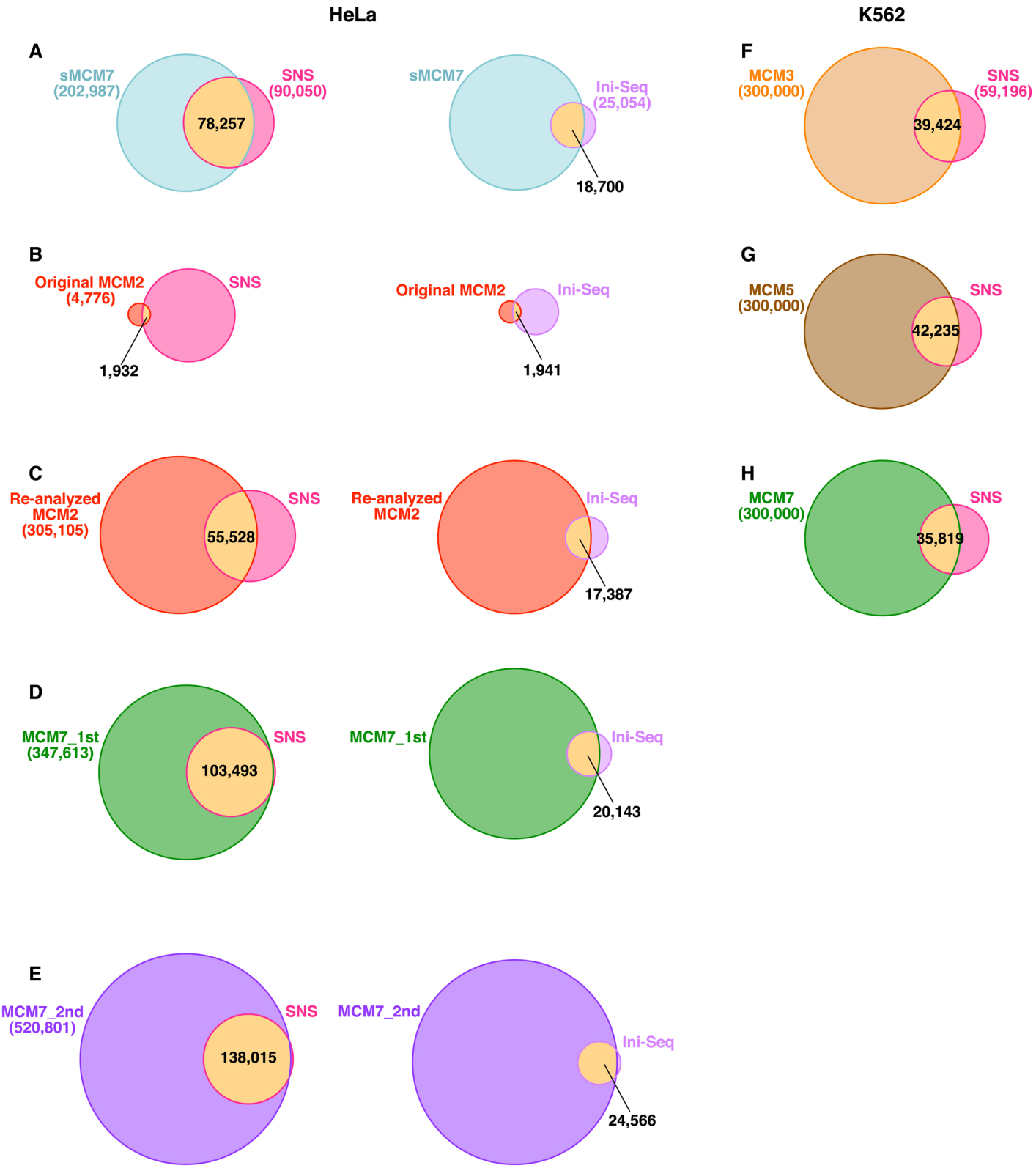

Supplemental Figure S5
Sugimoto et al.

Supplemental Table S1. Data sources used in this study.

Marks/Factors	GEO accession number or reference of the data	GEO accession number or reference for experimental condition	Note
MCM7_1st	(28)	(28)	Asynchronous HeLa cells
MCM7_2nd	This study	This study	Asynchronous HeLa cells
SNS-Seq	(13)	(13)	Asynchronous HeLa cells
SNS-Seq (Besnard)	(12)	(12)	Asynchronous HeLa cells
Ini-Seq	(40)	(40)	Cell-free system (EJ30 cell nuclei)
FAIRE-Seq	(28)	(28)	Asynchronous HeLa cells
DNase-Seq	GSM816633	GSE32970	Asynchronous HeLa cells
Repli-Seq	GSM923449	GSE34399	Asynchronous HeLa cells
H3K9ac	GSM733756	GSE29611	Asynchronous HeLa cells
H3K4me3	GSM733682	GSE29611	Asynchronous HeLa cells
H4K20me1	GSM733689	GSE29611	Asynchronous HeLa cells
H3K27me3	GSM733696	GSE29611	Asynchronous HeLa cells
H3K9me3	GSM1003480	GSE29611	Asynchronous HeLa cells
RNA-Seq	GSE33480	GSE33480	Asynchronous HeLa cells
E2F1	GSM935484	GSE31477	Asynchronous HeLa cells
c-myc	GSM935320	GSE31477	Asynchronous HeLa cells
ELK1	GSM935326	GSE31477	Asynchronous HeLa cells
Nrf1	GSM935636	GSE31477	Asynchronous HeLa cells
Nrf2	GSM803454	GSE32465	Asynchronous HeLa cells
MAZ	GSM935272	GSE31477	Asynchronous HeLa cells
c-Jun	GSM935341	GSE31477	Asynchronous HeLa cells
c-Fos	GSM935317	GSE31477	Asynchronous HeLa cells
STAT3	GSM935276	GSE31477	Asynchronous HeLa cells
TBP	GSM935606	GSE31477	Asynchronous HeLa cells
G4-Seq	(57)	(57)	Sequencing DNA from primary B lymphocytes under conditions that promote G4 formation in vitro
MCM2	(38)	(38)	Asynchronous HeLa cells
SNS-Seq	(13)	(13)	Asynchronous K562 cells
MCM3	GSM2424244	GSM2424244	Asynchronous K562 cells
MCM5	GSM2422960	GSM2422960	Asynchronous K562 cells
MCM7	GSM2422918	GSM2422918	Asynchronous K562 cells

Supplemental Table S2. Arbitrary classification of gene expression in HeLa cells into four classes based on FPKM values.

Class	FPKM	Number of genes
High expression	9.66 – 25917.7	7,122
Medium expression	1.48 – 9.66	7,122
Low expression	9.9138E-236 – 1.48	7,122
No expression	0	8,162

Supplemental Table S3. Outline of representative functions of transcription factors.

Transcription factor	Function	Reference
E2F1 and c-myc	Stimulation of the expression of the cell-cycle regulators; Stimulation of ORC recruitment	(89, 90)
ELK1	ETS family; Trans-activation of the cell-cycle regulatory gene *p21*	(91)
Nrf1	Redox-sensitive transcription factor; Binding to promoters of *Cdc2*, *PRC1*, *PCNA*, *cyclin B1* and *CDC25C* and controlling their expression	(92)
Nrf2	Pivotal factor for cell protection from oxidative and electrophilic insults; Regulation of the G1 to S phase transition by modulating the expression of *p21* and the *Rb*	(93)
MAZ	Zinc finger protein; Promotion of cyclin-dependent kinase inhibitor 1A (*CDKN1A*) expression; Regulation of *c-myc* transcription	(94, 95)
c-Jun and Fos	Forming dimer; Promotion of G1 to S phase transition by regulating the expression of the cell-cycle regulators	(96, 97)
STAT3	Latent transcription factors; Primarily mediating signalling from cytokine and growth factor receptors and promoting proliferation by stimulating transcription of *cyclin B1*, *Cdc2*, *c-myc* and *cyclin D1*	(98)

Supplemental Table S4. List of human genes known as CFSs with gene length and expression level (FPKM).

Gene	CFS	Gene length (kb)	FPKM
CNTNAP2	FRA7I	2304.6	0
DMD	FRAXC	2220.4	59.887
DLG2	FRA11F	2172.3	0.271
CSMD1	FRA8B	2059.5	0.002
LRP1B	FRA2F	1900.3	0.206
CTNNA3	FRA10D	1776.2	0.026
NRXN3	FRA14C	1697.9	0
FHIT	FRA3B	1502.1	0.029
MAGI2	FRA7E	1436.5	0
PARK2	FRA6E	1380.2	0.007
PRKG1	FRA10C	1307.2	0.008
DAB1	FRA1B	1252.6	0.085
CSMD3	FRA8C	1214.1	0.207
DCC	FRA18B	1195.7	0
AUTS2	FRA7J	1194.0	0
GPC6	FRA13D	1181.2	0
CTNNA2	FRA2E	1135.9	0.021
OPCML	FRA11G	1117.5	0
NRXN1	FRA2D	1114.0	0
WWOX	FRA16D	1113.2	4.083
CDH12	FRA5E	1102.8	0.022
IMMP2L	FRA7K	899.5	11.120
DPYD	FRA1E	843.3	9.899
RORA	FRA15A	741.0	0.347
NBEA	FRA13A	730.5	0.537
PAPPA	FRA9E	248.5	0.908
SMAD5	FRA5C	49.9	8.748
TES	FRA7G	48.3	19.145
PARP1	FRA1H	47.4	33.605
ZNF330	FRA4C	13.8	17.847
FZD5	FRA2I	6.8	1.359

Supplemental S5. Mean gene length and FPKM values of the 31 genes in the dataset.

	Annotation	Mean length (kb)	Mean FPKM
CFS	Supplemental Table S4	1129.3 ± 669	5.4 ± 12.7
LongGene_RS_1	Randomly selected 31 genes from long genes that are more than 700 kb in length	903.9 ± 215	0.8 ± 1.3
LongGene_RS_2	same as above	956.4 ± 212	2.2 ± 5.4
LongGene_RS_3	same as above	1066.0 ± 362	1.6 ± 3.4
Gene_RS_1	Randomly selected 31 genes from all genes	66.4 ± 116	29.2 ± 93.6
Gene_RS_2	same as above	63.4 ± 90	7.1 ± 15.7
Gene_RS_3	same as above	44.1 ± 77	8.9 ± 16.3

Supplemental Table S6. Compliance of qPCR experiments with the MIQE guidelines.

ITEM TO CHECK	IMPORTANCE	CHECKLIST	COMMENTS
Definition of experimental and control groups	E	✔	**Experimental groups**: anti-MCM7 ChIP. **Control groups**: Rabbit IgG ChIP.
Number within each group	E	✔	**LMNB2** or **MCM4:** n=8; **PAF1** or **LRIG2**: n = 4
Assay carried out by core lab or investigator's lab?	D	✔	Investigator's lab
Acknowledgement of authors' contributions	D	✔	NS performed qPCR.
Description	E	✔	Tissue culture cells
Volume/mass of sample processed	D	✔	$6x10^6$ cells / antibody
Microdissection or macrodissection	E	✔	Not applicable
Processing procedure	E	✔	Not applicable
If frozen - how and how quickly?	E	✔	Not applicable
If fixed - with what, how quickly?	E	✔	Not applicable
Sample storage conditions and duration (especially for FFPE samples)	E	✔	Not applicable
Procedure and/or instrumentation	E	✔	After formaldehyde reversal, the samples were serially treated with DNase-free RNase A (final 5 µg, Invitrogen) and Proteinase K (final 50 µg/ml, Roche). The DNA was phenol:chloroform (Nacalai tesque) extracted, ethanol (Nacalai tesque) precipitated in the presence of 1 µl of glycogen (Nacalai tesque), and dissolved in Tris/EDTA buffer.
Name of kit and details of any modifications	E	✔	We did not use any kit.
Source of additional reagents used	D		Not applicable
Details of DNase or RNAse treatment	E	✔	RNase (5 µg, Invitrogen) was added and incubated at 37°C for 30 min.
Contamination assessment (DNA or RNA)	E		Not performed
Nucleic acid quantification	E	✔	Using the ratio of 260 nm/280 nm
Instrument and method	E	✔	Nanodrop (Thermo Scientific)
Purity (A260/A280)	D	✔	1.8 – 1.9
Yield	D	✔	The mean yield of input DNA was 660 µg/ml, with a minimum value of 532 µg/ml and a maximum value of 877 µg/ml.
RNA integrity method/instrument	E	✔	Not applicable
RIN/RQI or Cq of 3' and 5' transcripts	E	✔	Not applicable
Electrophoresis traces	D	✔	Not applicable
Inhibition testing (Cq dilutions, spike or other)	E	✔	Not applicable
Complete reaction conditions	E	✔	Not applicable
Amount of RNA and reaction volume	E	✔	Not applicable
Priming oligonucleotide (if using GSP) and concentration	E	✔	Not applicable
Reverse transcriptase and concentration	E	✔	Not applicable
Temperature and time	E	✔	Not applicable
Manufacturer of reagents and catalogue numbers	D	✔	Not applicable
Cqs with and without RT	D	✔	Not applicable
Storage conditions of cDNA	D	✔	Not applicable
If multiplex, efficiency and LOD of each assay.	E	✔	Not applicable
Sequence accession number	E	✔	**LMNB2**: NM_032737.3; **MCM4**: NG_032967.1; **PAF1**: AC104106.2; **LRIG2**: NG_042819.1
Location of amplicon	D	✔	See Sugimoto et al., Nucleic Acids Research, 43: 5898-5911, 2015. doi: 10.1093/nar/gkv
Amplicon length	E	✔	**LMNB2 ori**: 232 bp; **LMNB2 distal**: 240 bp; **MCM4 ori**: 215 bp; **MCM4 distal**: 209 bp; **PAF1 ori**: 80 bp; **PAF1 distal**: 130 bp; **LRIG2 ori**: 118 bp; **LRIG2 distal**: 127 bp
In silico specificity screen (BLAST, etc)	E	✔	We confirmed all primers by BLAST.
Pseudogenes, retropseudogenes or other homologs?	D		
Sequence alignment	D		
Secondary structure analysis of amplicon	D		
Location of each primer by exon or intron (if applicable)	E	✔	Not applicable
What splice variants are targeted?	E	✔	Not applicable
Primer sequences	E	✔	**LMNB2 ori Forward:** ggctggcatggactttcatttcag, **Reverse:** gtggagggatctttcttagacatc; **LMNB2 distal Forward:** gttaacagtcaggcgcatgggcc, **Reverse:** ccatcagggtcacctctggttcc; **MCM4 ori Forward:** ggacattacagatgcatttctc, **Reverse:** aagagttccaagtttgttcctc; **MCM4 distal Forward:** tacctgtgggtaagagatgagttg, **Reverse:** ctctatacatgcaacgacttggg; **PAF1 ori Forward:** tcggaaccacacacggattg, **Reverse:**ctctccaccaatcacagaagca; **PAF1 distal Forward:** agtgtgctgagtacctggtttc, **Reverse:** attgctcgggagtacaactgg; **LRIG2 ori Forward:** actgcagtcgcaggaaattg, **Reverse:** ctccccctcctttggtcac; **LRIG2 distal Forward:** tggaacatcagcttggaatcac, **Reverse:** gcatctctggattaaacatcccac
RTPrimerDB Identification Number	D	✔	Not applicable
Probe sequences	D	✔	Not applicable
Location and identity of any modifications	E	✔	Not modified
Manufacturer of oligonucleotides	D	✔	**LMNB2 and MCM4:** FASMAC; **PAF1 and LRIG2:** SIGMA
Purification method	D	✔	**LMNB2 and MCM4:** Reversed-phase chromatography; **PAF1 and LRIG2:** OPC purification
Complete reaction conditions	E	✔	PCR reactions were performed in a CFX96 Real-Time PCR Detection system (Bio-Rad) using SYBR Premix EX Taq II (Takara) in final volume of 25 µl. Reaction mix consisted of sterile H_2O MilliQ, 12.5 µl 2x SYBR Premix ExTaq II, 1µl 5µM each forward and reverse primers and 1 µl ChIPed-DNA.
Reaction volume and amount of cDNA/DNA	E	✔	Reaction volume: 25 µl; amount of ChIPed DNA: 1 µl
Primer, (probe), Mg++ and dNTP concentrations	E	✔	200 nM primers
Polymerase identity and concentration	E	✔	Manufactures proprietary
Buffer/kit identity and manufacturer	E	✔	SYBR Premix EX Taq II (Takara)
Exact chemical constitution of the buffer	D	✔	Manufactures proprietary
Additives (SYBR Green I, DMSO, etc.)	E	✔	No additives
Manufacturer of plates/tubes and catalog number	D	✔	96-well plates (SKPCR96C) and PCR Strip Caps (SKPCR8FC), both provided by SEIKO Co. LTD (Japan).
Complete thermocycling parameters	E	✔	**LMNB2 and MCM4:** 1 min at 95°C; five cycles at 95°C for 30 sec, annealing temparature plus 4°C for 30 sec, and 72°C for 30 sec, five cycles at 95°C for 30 sec, anneaing temparature plus 2°C for 30 sec, and 72°C for 30 sec; and 50 cycles at 95°C for 30 sec, anneling temparature for 30 sec, and 72°C for 30 sec. **PAF1 and LRIG2:** 1 min at 95°C; and 50 cycles at 95°C for 30 sec, anneling temparature for 30 sec, and 72°C for 30 sec. The annealing temparatures were set as follows: **LMNB2 ori**: 62.9°C; **LMNB2 distal**: 67.1°C; **MCM4 ori**: 55.1°C; **MCM4 distal**: 65.5°C; **PAF1 ori and PAF1 distal**: 60.2°C; **LRIG2 ori and LRIG2 distal**: 59.8°C
Reaction setup (manual/robotic)	D	✔	Manual setup
Manufacturer of qPCR instrument	E	✔	CFX96 Real-Time PCR Detection system (Bio-Rad)

Evidence of optimisation (from gradients)	D	✔	None
Specificity (gel, sequence, melt, or digest)	**E**	✔	Melting curve analysis, ramping from 72°C to 95°C in steps of 0.5°C, where fluorescence data are measured continously. Gene-specific amplification was confirmed by a single band in 3% agarose gel electrophoresis stained with ethidium bromide. No template controls (no cDNA in PCR) were run for each gene to detect unspecific amplification and primer dimerization.
For SYBR Green I, Cq of the NTC	**E**	✔	> 40 or no amplification
Standard curves with slope and y-intercept	**E**	✔	Representative values are shown. **LMNB2 ori:** y = -3.162x + 26.675; **LMNB2 distal:** y = -3.239x + 26.882; **MCM4 ori:** y = -3.366x + 28.005; **MCM4 distal:** y = -3.212x + 29.118; **PAF1 ori:** y = -3.555x + 41.135; **PAF1 distal:** y = -3.253x + 40.52; **LRIG2 ori:** -3.35x + 40.243; **LRIG2 distal:** y = -3.256x + 40.106
PCR efficiency calculated from slope	**E**	✔	**LMNB2 ori:** 82.688 – 127.65%; **LMNB2 distal:** 82.86 – 121.53%; **MCM4 ori:** 80.75 – 117.52%; **MCM4 distal:** 78.52 – 109.72%; **PAF1 ori:** 89.57 – 115.38%; **PAF1 distal:** 84.18 – 109.28%; **LRIG2 ori:** 91.46 – 128.26%; **LRIG2 distal:** 95.11 – 110.99%
Confidence interval for PCR efficiency or standard error	D		
r2 of standard curve	**E**	✔	**LMNB2 ori:** 0.98 – 1.0; **LMNB2 distal:** 0.993 – 1.0; **MCM4 ori:** 0.982 – 1.0; **MCM4 distal:** 0.988 – 1.0; **PAF1 ori:** 0.986 – 0.999; **PAF1 distal:** 0.982 – 0.998; **LRIG2 ori:** 0.981 – 0.999; **LRIG2 distal:** 0.990 – 0.998
Linear dynamic range	**E**	✔	The Cq values of unknown samples fell within the linear range.
Cq variation at lower limit	**E**	✔	Not performed
Confidence intervals throughout range	D	✔	Not performed
Evidence for limit of detection	**E**	✔	Not performed
If multiplex, efficiency and LOD of each assay.	**E**	✔	Not applicable
qPCR analysis program (source, version)	**E**	✔	CFX Manager Software (Bio-Rad), version 3.1
Cq method determination	**E**	✔	The CFX software Single Threshold mode was used to determine Cq for each gene
Outlier identification and disposition	**E**	✔	None of the Cq values was discarded
Results of NTCs	**E**	✔	> 40 or no amplification
Justification of number and choice of reference genes	**E**	✔	Not applicable
Description of normalisation method	**E**	✔	Standard curve quantification
Number and concordance of biological replicates	D	✔	**LMNB2 or MCM4:** n=4; **PAF1 or LRIG2:** n = 2
Number and stage (RT or qPCR) of technical replicates	**E**	✔	qPCR reactions were performed in duplicate
Repeatability (intra-assay variation)	**E**	✔	Standard deviation of duplicates: 0.002 – 0.04
Reproducibility (inter-assay variation, %CV)	D		
Power analysis	D		
Statistical methods for result significance	**E**	✔	Student's t-test
Software (source, version)	**E**	✔	Microsoft Excel version 14.7.3
Cq or raw data submission using RDML	D		

SUPPLEMENTAL REFERENCES

89. Bosco,G., Du,W. and Orr-Weaver,T.L. (2001) DNA replication control through interaction of E2F-RB and the origin recognition complex. *Nat. Cell Biol*., **3**, 289–295.

90. Dominguez-Sola,D., Ying,C.Y., Grandori,C., Ruggiero,L., Chen,B., Li,M., Galloway,D.A., Gu,W., Gautier,J. and Dalla-Favera,R. (2007) Non-transcriptional control of DNA replication by c-Myc. *Nature*, **448**, 445–451.

91. Shin,S.Y., Kim,C.G., Lim,Y. and Lee,Y.H. (2011) The ETS family transcription factor ELK-1 regulates induction of the cell cycle-regulatory gene p21(Waf1/Cip1) and the BAX gene in sodium arsenite-exposed human keratinocyte HaCaT cells. *J. Biol. Chem*., **286**, 26860–26872.

92. Okoh,V.O., Garba,N.A., Penney,R.B., Das,J., Deoraj,A., Singh,K.P., Sarkar,S., Felty,Q., Yoo,C., Jackson,R.M., et al. (2015) Redox signalling to nuclear regulatory proteins by reactive oxygen species contributes to oestrogen-induced growth of breast cancer cells. *Br. J. Cancer*, **112**, 1687–1702.

93. Homma,S., Ishii,Y., Morishima,Y., Yamadori,T., Matsuno,Y., Haraguchi,N., Kikuchi,N., Satoh,H., Sakamoto,T., Hizawa,N., et al. (2009) Nrf2 enhances cell proliferation and resistance to anticancer drugs in human lung cancer. *Clin. Cancer Res*., **15**, 3423–3432.

94. Ugai,H., Li,H.O., Komatsu,M., Tsutsui,H., Song,J., Shiga,T., Fearon,E., Murata,T. and Yokoyama,K.K. (2001) Interaction of Myc-associated zinc finger protein with DCC, the product of a tumor-suppressor gene, during the neural differentiation of P19 EC cells. *Biochem. Biophys. Res. Commun*., **286**, 1087–1097.

95. Ray,A., Shakya,A., Kumar,D. and Ray,B.K. (2004) Overexpression of serum amyloid A-activating factor 1 inhibits cell proliferation by the induction of cyclin-dependent protein kinase inhibitor p21WAF-1/Cip-1/Sdi-1 expression. *J. Immuno*l. (Baltimore, Md. 1950), **172**, 5006–5015.

96. Ryseck,R.P., Hirai,S.I., Yaniv,M. and Bravo,R. (1988) Transcriptional activation of c-jun during the G0/G1 transition in mouse fibroblasts. *Nature*, **334**, 535–537.

97. Kovary,K. and Bravo,R. (1991) The jun and fos protein families are both required for cell cycle progression in fibroblasts. *Mol. Cell. Biol*., **11**, 4466–4472.

98. Jarnicki,A., Putoczki,T. and Ernst,M. (2010) Stat3: linking inflammation to epithelial cancer - more than a ‘gut’ feeling? *Cell Div*., **5**, 14.